aerospace

MDPI

Article

Optimization of Land-Based Impact Zones for Spent Rocket Stages Launched from the Baikonur Cosmodrome

Gulnaz Yermoldina [1,2,3,*], Aliya Yskak [3], Nurlan Suimenbayev [4] and Elmira Yermoldina [5]

[1] Aerospace Technologies Laboratory, Institute of Information and Computational Technologies, 050010 Almaty, Kazakhstan
[2] Faculty of Mechanics and Mathematics, Kazakh National University Named After Al-Farabi, 050040 Almaty, Kazakhstan
[3] Research Institute of Innovative Technologies, Akhmet Baitursynuly Kostanay Regional University, 110000 Kostanay, Kazakhstan; aliy.yskak@gmail.com
[4] National Centre of Space Research and Technology, 050000 Almaty, Kazakhstan; n.suimenbayev@gmail.com
[5] Branch Office of the Republican State Enterprise "Infracos", 050046 Almaty, Kazakhstan; eermoldina@gmail.com
* Correspondence: gulnazyermoldina@gmail.com

Abstract

The article presents a comprehensive methodology for optimizing ground impact zones of spent rocket stages based on the integration of geoinformation analysis, remote sensing of Earth, ballistic modeling, and ecosystem sustainability assessment. An information and analytical system (IAS) has been developed and tested, providing automated selection of environmentally sustainable landing points within acceptable dispersion zones. The methodology includes the use of the NDVI, digital terrain models, soil quality assessments, fire hazard assessments, and environmental damage calculations. For the first time, a system for classifying operational-territorial units according to their level of resilience to man-made impacts has been formed. The results suggest the potential for the reduction of the dangerous impact zone under modeled conditions. The system architecture is designed to be scalable and applicable to other spaceports located in continental regions. The presented methodology contributes to the development of an environmentally oriented approach to aerospace infrastructure management.

Keywords: controlled descent; environmental safety; launch vehicles; impact areas; information and analytical system; operational-territorial unit

Check for updates

Academic Editor: Vladimir S. Aslanov

Received: 18 May 2026
Revised: 7 June 2026
Accepted: 10 June 2026
Published: 25 June 2026

Copyright: © 2026 by the authors. Licensee MDPI, Basel, Switzerland. This article is an open access article distributed under the terms and conditions of the Creative Commons Attribution (CC BY) license.

1. Introduction

Space rockets affect virtually all of Earth's geospheres and its surface up to geostationary orbits. The impact on the environment is very diverse: acoustic, thermal, mechanical, chemical, and radioactive. In some cases, these types of impacts are interrelated, and their contribution to the overall disturbance depends on the type of launch vehicle, flight altitude, equipment operation, emergency situations, and the technology used in the rocket and space complex.

Spacecraft launches are always accompanied by the fall of detachable parts of launch vehicles (LVs) to the ground. These include spent stages, payload fairings, and connecting compartments that ensure the launch of the rocket. The size and location of the fall areas for these parts for each route are determined by the requirements for spacecraft orbits, their mass, and the energy characteristics of the rockets, and are selected, where possible, in areas with the lowest population density and minimal economic activity.

In Russia and Kazakhstan, the location of spaceports is such that significant areas of the fall zones of spent launch vehicle stages are located on their own land territory. Unlike Russia and Kazakhstan, where spent rocket stages often fall on land, the main fall zones for countries such as the United States, the European Union, Japan, India, and Brazil are often located over oceanic areas. However, this does not eliminate environmental safety issues entirely but rather shifts them toward marine ecosystems. Thus, oceanic and continental landfalls present different environmental challenges. The development of reusable and controlled descent systems, such as those used by SpaceX, offers an effective way to mitigate both types of impacts.

The problem of contamination of large areas where the first stages of launch vehicles fall with unused residues of toxic rocket fuel components (RFC) has always been and remains a pressing issue for Kazakhstan [1,2]. The solution to this problem has so far mainly consisted of decontaminating the sites of spills of highly toxic rocket fuel components.

The problem of optimizing and reducing the landing areas of first stages of rockets becomes particularly relevant in the case of their deployment on land, especially when it comes to newly developed areas. For example, to ensure the launch of the Soyuz-2 rocket from the Baikonur cosmodrome along a new route in a northerly direction to near-polar orbits, a new area of about 6000 hectares has been opened in the Kostanay region of the Republic of Kazakhstan for the fall of separable parts of the launch vehicle [3].

Among the most significant adverse environmental factors are gaseous emissions [4], ozone-depleting substances [4,5], mechanical contamination by stage fragments and residual propellants, as well as pollution of soil, water, air, and vegetation by toxic rocket propellants (RP) [6]. Fuel degradation products have been detected at concentrations significantly exceeding permissible limits [6]. These compounds are capable of accumulating, migrating, and transforming into even more toxic substances, eventually entering the human body through food chains [7].

Studies of the first-stage impact zones of the Proton-M launch vehicle have revealed suppression of vegetation cover, low species diversity, and prolonged ecological succession periods [1]. Soil microbial communities are also adversely affected, as evidenced by low biochemical oxygen demand and minimal cellulase activity [8], reducing the soil's self-purification capacity and leading to a decline in fertility [9,10].

In the event of launch failures, the scale of environmental damage increases dramatically [8,11], resulting in the expansion of ecological disturbance areas, destruction of soil and vegetation cover, and the occurrence of wildfires [7,10]. Mechanical impacts associated with Proton stage falls include crater formation, dispersion of large fragments over areas exceeding 1200 m^2 and small fragments over more than 22,000 m^2, vegetation fires affecting over 245,000 m^2, and spills of propellants (nitrogen tetroxide and UDMH) covering up to 737 m^2 [9]. For Soyuz strap-on boosters, debris dispersion areas range from 325 to 43,627 m^2, fire-affected areas exceed 8000 m^2, and fuel spill areas reach up to 129 m^2 [8]. To mitigate these impacts, various detoxification methods have been proposed [12], along with rapid detection and recovery systems for fallen rocket fragments [13].

During a nominal Proton launch, approximately 2.6 tons of unused propellant are intentionally vented, whereas launch failures may release tens of tons of toxic fuel directly into natural ecosystems. According to the lease agreement [14], 51 designated impact areas with a total area exceeding 4.14 million hectares have been allocated for falling rocket stages.

Rocket launches affect the environment both within the cosmodrome area and at the locations where separated rocket stages fall along the flight trajectory. These impacts include both environmental effects specific to rocket and space activities and general industrial environmental impacts [15,16].

Studies of the impact zones associated with Soyuz and Proton launch vehicles indicate contamination of atmospheric air, water bodies, and soils, as well as the accumulation of pollutants in ecosystem components. Numerous investigations have confirmed the presence of rocket fuel components in environmental media and biota, depletion of stratospheric ozone, degradation of soil properties, and reductions in vegetation biodiversity [1,2,4–13,15–21].

An assessment of the current condition of stage impact areas highlights the need for new approaches to ensuring the environmental safety of cosmodrome ground infrastructure. Studies [22,23] propose measures aimed at improving the detection of rocket fragments, developing infrastructure for their collection and storage, creating technical detection systems, establishing comprehensive environmental monitoring programs, and enhancing coordination among relevant organizations.

Other studies have explored improvements in environmental safety through the advancement of propulsion and control systems [23,24], the use of less toxic propellants, optimization of stage design and flight trajectories [25], and the development of reusable launch vehicles [26–29]. In recent years, interest in reusable space transportation systems has increased worldwide [30,31]. One of the most effective solutions is the controlled descent and recovery of spent rocket stages [18,32–38].

Studies [24,33–35,39] propose equipping rocket stages with controlled descent systems that enable landing at predetermined locations. This approach substantially reduces the size of impact zones and improves the environmental safety of affected territories [36–43]. Nevertheless, existing environmental requirements remain largely limited to recommendations concerning the elimination of toxic propellant components [8,17,22]. Consequently, the optimization of rocket stage impact areas and the assessment of associated environmental damage have become particularly important research challenges [40]. Addressing these challenges requires the development of effective tools for predicting landing locations and evaluating the environmental condition of potential landing sites.

The scientific novelty of this study lies in the development of an integrated methodology for predicting spent rocket stage landing locations through the combination of geospatial analysis, remote sensing, ballistic modeling, and environmental resilience assessment. For the first time, an Information and Analytical System (IAS) architecture is proposed to support the automated selection of optimal landing sites within permissible dispersion ellipses. The methodology incorporates NDVI data, digital elevation models, soil characteristics, wildfire hazard indicators, and ecosystem restoration costs.

The study forms a new direction in aerospace technology–environmentally oriented management of rocket LV fall zones. The results obtained make it possible to reduce the fall zone area, while preserving the stability of natural landscapes and minimizing the technogenic load.

This research combines optimization and reduction of the rocket stage fall area to develop recommendations for design solutions and design parameters of the launch vehicle. To this end, it is proposed to develop an IAS that takes into account compliance with environmental safety standards. The proposed optimization architecture allows identifying and determining the predicted landing points of the LV stages, taking into account the selection of sustainable areas and the economic assessment of the costs of restoring ecosystems. The system is designed to support the identification of alternative landing sites, the assessment of their environmental sustainability, and the minimization of environmental impacts while maintaining the required launch safety parameters.

2. Setting the Research Task

The concept of controlled descent of spent launch vehicle stages involves the development of technologies for selecting landing sites that are resistant to mechanical and

pyrogenic–thermal loads. Using residual propellant, separated stages perform a guided descent to a predefined point within the impact area, thereby preventing fires and explosions, reducing the size of drop zones, and eliminating chemical contamination of the environment [41,42].

The novelty of this concept lies in its integrated approach, which combines the development of controlled descent systems, methodologies for selecting the most environmentally and technically resilient landing sites, and the assessment of descent maneuvers based on impact zone calculations and landing performance analysis of the stages [43–47]. Consequently, the development of an automated methodological framework for identifying optimal landing areas within designated impact zones represents an important research and engineering challenge.

To address this challenge, a specialized Information and Analytical System (IAS) is required, capable of selecting optimal landing sites while considering topography, geological conditions, technogenic risks, and the effects of thermal and mechanical energy on the landscape. The implementation of such a system will improve the accuracy of landing site prediction, reduce the extent of hazardous areas, and enhance both environmental and industrial safety in territories adjacent to the Baikonur Cosmodrome. The interaction between the cosmodrome IAS and the launch vehicle should be iterative in nature. At the current stage, the primary objective is the development of the impact-area Information and Analytical System (IASia) and a database of potentially suitable landing sites for each impact zone. The resulting data are required for (a) synthesizing launch vehicle guidance programs without imposing landing-site constraints; (b) assessing deviations between actual and recommended landing points; and (c) developing recommendations for improving stage technical characteristics to support controlled descent maneuvers (Figure 1).

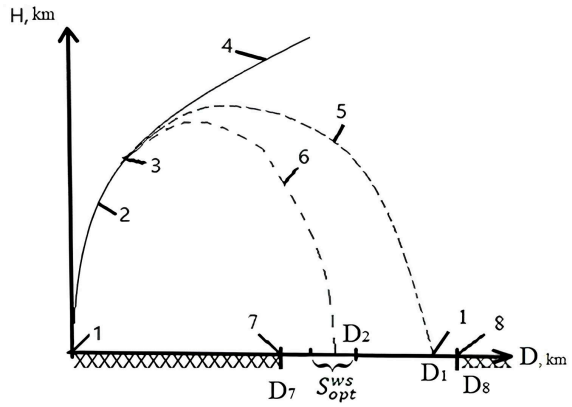


Figure 1. Optimization of the spent stage flight path within the framework of the controlled descent concept. 1—start point of the launch vehicle; 2—the active section of the launch vehicle first stage injection trajectory; 3—spent stage separation; 4—active section of the launch vehicle second stage injection trajectory; 5—the ballistic trajectory of the spent stage descent corresponds to the energy-optimal launch trajectory of the first stage, and the spent stage landing point is located at a distance D_1, from the start point of the launch vehicle; 6—the trajectory of the controlled landing of the spent stage into the selected zone S_{opt}^{ws}, the centre of which is located at a distance D_2 from the start point of the LV_1; 7—the beginning of the LA territory corresponding to the range D_7 from the launch point LV_1; 8—the end of the impact area corresponding to the range D_8 from the launch point LV_1.

Traditional impact zones for separated rocket stages at the Baikonur Cosmodrome are characterized by extensive spatial coverage, uncertainty in landing locations, and insufficient consideration of environmental vulnerability. This increases the risk of soil and vegetation degradation, contamination by residual rocket propellants, and the costs associated with environmental remediation.

Previous studies [8–13,36,40,43] have primarily focused on the ballistic and technical aspects of LV stage separation, emphasizing trajectory control and flight safety. Considerably less attention has been paid to the integration of environmental sustainability into impact zone design [48,49], resulting in a methodological gap between aerospace engineering practices and environmental management.

This study proposes a concept that integrates geoinformation analysis, remote sensing of Earth (RSE) data, and environmental sustainability modeling into a unified Information and Analytical System (IAS). The system enables the automated identification of environmentally preferable controlled descent zones based on quantitative spatial data. The main objectives of the study are as follows:

- Formalization of environmental and geotechnical criteria for assessing the sustainability of territories affected by LV operations;
- Development of a modular IAS architecture integrating RSE and GIS datasets with multicriteria ranking methods;
- Development and validation of a spatial assessment framework for evaluating the sustainability of operational-territorial units within the impact areas of the Baikonur Cosmodrome;
- Assessment of the applicability of the IAS for environmentally safe planning of impact zones at other national spaceports.

Unlike conventional approaches based primarily on ballistic dispersion modeling and safety distance calculations, where environmental factors are treated as secondary considerations [40], the proposed methodology directly incorporates ecosystem sustainability indicators into the decision-making process for selecting controlled descent zones. This makes it possible to account for soil sensitivity, vegetation conditions, and potential pollutant migration risks during the planning stage rather than after impact events have occurred.

The conceptual and methodological assumptions outlined above formed the basis for the development of the IAS, its data structure, and the analytical procedures used.

3. Materials and Methods

The methodological basis includes a combination of ballistic modeling, geoinformation analysis, and assessment of the ecological sustainability of territories.

The architecture of the information and analytical system (IAS) combines diverse spatial data (vegetation, soil, relief, hydrology, meteorological parameters) into a single platform for calculating and visualizing areas of environmental sustainability.

The structure of the information and analytical system (IAS) consists of four interconnected subsystems:

(1) A GIS database storing spatial and attribute data;
(2) An “Accuracy” database including ballistic modeling parameters and dispersion ellipses;
(3) A “Toxicity” database describing the potential chemical risks from fuel residues;
(4) An “Eco-passport” database aggregating indicators of the environmental condition of the impact area for authorized bodies (the Ministry of Ecology and Natural Resources of the Republic of Kazakhstan).

The schematic structure of the IAS for the impact area (IASia) is shown in Figure 2.

Together, these components create a modular structure that allows engineering, geographical, and environmental factors to be considered jointly in a single computing environment.

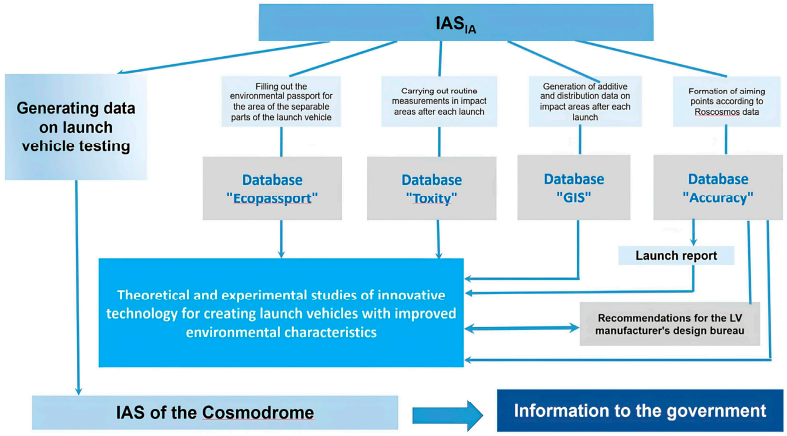


Figure 2. Architecture of the Information and Analytical System (IAS) for rocket stage impact zones.

Optimization of the spent stage drop zone—the focus of our research—is stored in the GIS database.

Methodologically, the GIS database combines several thematic layers: vegetation condition, soil mechanical strength, soil ecological quality, and relief-hydrological stability. Each of these contributes to the overall assessment of OTU sustainability, forming the basis for a balanced multi-criteria analysis that supports both environmental assessment and operational planning.

Considering the potential adverse environmental impacts associated with launch vehicle operations and the requirement to certify each impact zone [45], the design of landing areas with resilient ecosystem characteristics should be based on constraining the fragment dispersion area using a calculated ellipsoid, developing a geospatial database, and conducting a comprehensive assessment of environmental sustainability that accounts for natural, climatic, topographic, socio-economic, and infrastructural factors, as well as potential environmental and economic damage.

To address the issue of environmental safety at these rocket stage landing sites, it is necessary to identify the characteristics of ecosystem resilience and vulnerability to the impact of liquid-fuel launch vehicles.

The parameters of the stability and vulnerability of ecosystems (biogeocenoses) consist of the stability parameters of the main components: soil, water, and vegetation cover.

Therefore, to ensure environmental safety, it is necessary to take into account the factors of ecosystem stability in the landing area:

(a) Meteorological factors and vegetation flammability;
(b) Changes in soil quality, as well as deterioration of fertility and degradation;
(c) The state of vegetation cover;
(d) The presence of watercourses and the type of economic activity.

The general sequence of the study includes the following main stages:

- Collection and systematization of initial data;
- Modeling or operating with existing ballistic dispersion ellipses for selected types of missiles;
- Zoning of the territory and formation of operational-territorial units (OTU);
- Calculation of environmental sustainability indicators: state of vegetation (Q_{Vi}), fire hazard assessment (Q_{Fi}), soil strength (Q_{Si}), soil cover quality (Q_{Bi}), terrain relief (Q_{relief});
- Ranking of zones by degree of environmental sustainability;
- Interpretation of results and formulation of proposals for environmentally safe planning.

IAS combines diverse geospatial datasets to assess environmental stability in rocket launch fallout zones. Open and national geospatial data sources were used to conduct the study:

- Multispectral satellite imagery: Sentinel-2 Level-2A scenes (2017–2023) covering the growing season (May–September);
- Digital elevation model: ASTER GDEM v3 with a spatial resolution of 30 m for analyzing slopes, exposure, and hydrographic networks;
- Soil and environmental maps: datasets from the national digital soil and environmental survey at a scale of 1:200,000;
- Climate and reference data (including seasonality);
- Topographic and hydrographic layers: digitized from official maps and verified using remote sensing to refine contours, economic and water features.

All datasets were converted to UTM Zone 43 N (EPSG: 32643) projection and harmonized in terms of spatial resolution to ensure consistency between IAS modules. The study area is drop zone No. 15, 25 in the Ulytau district of the Karaganda region. The fall area has the shape of a double ellipse superimposed on each other. The geographical extent of the study area and its topographic base are shown in Figure 3. The contour outlined by a double ellipse in all figures visualizes the boundaries of the first stage impact area. This area is the subject of the present study, and all presented estimates pertain to it.

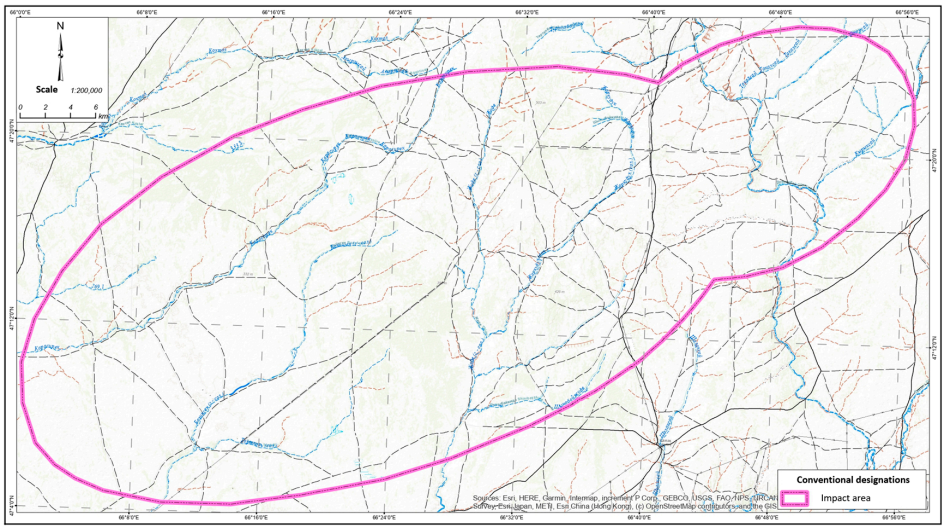


Figure 3. Topographic map of the area of impact No. 15.25 with the boundaries of the study area highlighted.

Sentinel-2 pre-processing (atmospheric correction, NDVI compositing) was performed using ESA SNAP 9.0 with the Sen2Cor 2.9 plugin. Cartographic processing and visualization were performed in ArcGIS Pro 3.x (ESRI, Redlands, CA, USA).

To ensure comparability and analytical correctness, the following preprocessing steps were applied to the input data:

- Atmospheric and radiometric correction of Sentinel-2 imagery;
- Cloud masking and generation of seasonal NDVI composites;
- Smoothing of temporal series (seasonal averaging for 2017–2023);
- Spatial resolution normalization (30 m × 30 m);
- Boundary clipping to the Yu-24 zone (Impact Areas No. 15 and No. 25);
- Creation of a regular (or irregular) analytical grid of 1 × 1 km (OTU), matching the boundaries of the study area.

Each grid element was assigned a unique identifier, which serves as a key for linking all thematic layers within the IGD geospatial database. The methods used are based on open sources and standards. Access restrictions apply only to operational field observations within the closed areas of the Yu-24 zone.

3.1. Determination of Impact Zones

The determination of rocket launch vehicle (LV) impact zones is a fundamental step in the development of the Information and Analytical System (IAS).

The most important aspect of justifying the choice of landing sites should be to minimize the negative impact on the environment and the population of adjacent territories.

Analysis of various cases of spent rocket stages landing in designated areas indicates the local nature of the impact of launches and differences in the intensity of the negative load on individual areas.

Ballistic fall zones are calculated using the Monte Carlo method, taking into account variations in stage separation parameters: height, angle of inclination, velocity vector, and aerodynamic drag [40]. For the Proton rocket, statistical dispersion ellipses are used. These ellipses are loaded into the IGD and used as spatial boundaries for assessing environmental parameters within the probable fall zones.

This approach to modeling provides a statistically reliable basis for determining fall zones under nominal launch conditions.

The orientation of the ellipses was tied to the flight azimuths of representative Proton launch trajectories, which ensured that the spatial model corresponded to actual operating conditions. The dispersion ellipses were imported into the IAS GIS database and overlaid on topographic and environmental datasets (vegetation, soil, relief, hydrology).

This integration allows automatic extraction of environmental parameters for each potential landing point and supports subsequent ranking of OTUs by stability and risk.

Each ellipse was referenced to the Baikonur coordinate system and divided into an irregular or regular grid. In this case, the grid corresponds to OTU cells (1 × 1 km). For each cell, IAS records the probability of its belonging within the impact ellipse, which allows for the subsequent calculation of area-weighted environmental indices (Figure 4).

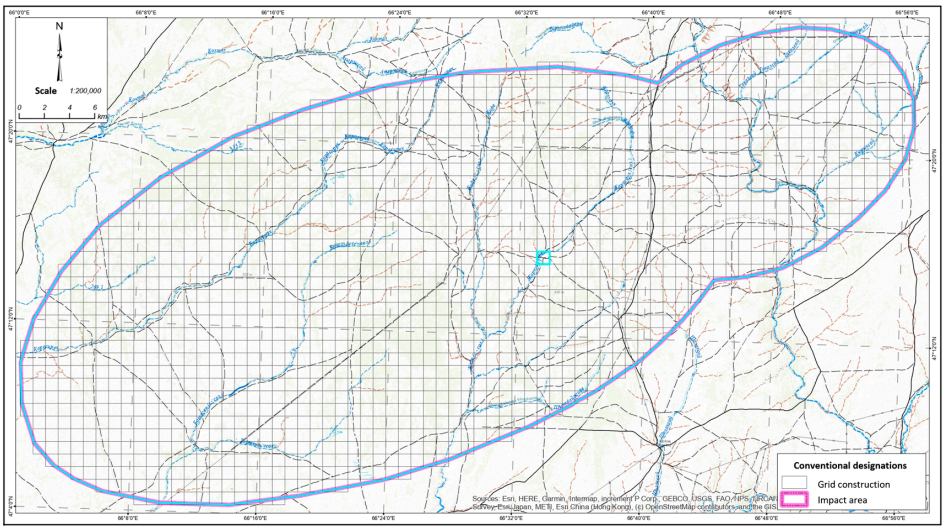


Figure 4. Creation of a grid from 1000 × 1000 m to delineate OTU within the affected area.

This spatial quantitative assessment links the probability of mechanical impact with environmental sensitivity, forming a unified assessment area for controlled descent planning.

Through this integration, the system transforms purely mechanical trajectory data into geo-ecological planning information, ensuring that flight safety and environmental stability are assessed within a single analytical framework.

3.2. Determination of Sustainable OTUs

Determining the most suitable OTU types involves the following steps [43]:

(1) A rectangular coordinate grid of n sections is superimposed on a topographic map of the study area of the proposed impact zone. Each section has a specific area of dimension Si and a unique ecotope composition (including soil and subsoil type, vegetation type, presence of water sources, etc.). It is also possible to rank the territory based on an irregular grid.

(2) Based on reference and normative indicators, topographic and thematic maps, Earth remote sensing data, inventory data from environmental passports, and methods for environmental assessment of territories [9], a database is created to evaluate the values of the specified criteria.

(3) Determination of vegetation cover sustainability: Vegetation data were obtained from Sentinel-2 images. Atmospheric and radiometric correction were performed using the ESA Sen2Cor 2.9 processor with standard L2A processing parameters. Image selection criteria included cloud cover $\leq 10\%$, temporal consistency during the growing season, and minimal atmospheric artifacts. A comprehensive list of all Sentinel-2 Level-2A scenes used in this study, including acquisition dates, scene identifiers, cloud-cover percentages, and quality flags, is provided in Table 1.

Table 1. Sentinel-2 Scenes Used in the Study (2017–2023).

Year	Acquisition Date	Scene ID (Tile/Format)	Cloud Cover (%)	Quality Flags Applied	Notes
2017	15 June 2017	S2A_MSIL2A_20170615T062621_T43UDQ	4.2	Cloud mask, saturation mask	Core scene, early vegetation season
2017	2 August 2017	S2B_MSIL2A_20170802T062629_T43UDQ	3.8	Cloud mask	Used for seasonal NDVI composite
2018	19 July 2018	S2A_MSIL2A_20180719T062621_T43UDQ	6.1	Cloud mask	Peak vegetation reference scene
2018	10 September 2018	S2B_MSIL2A_20180910T062619_T43UDQ	7.0	Cloud mask	Complementary lateseason data
2019	25 June 2019	S2A_MSIL2A_20190625T062631_T43UDQ	1.9	Cloud mask	High-quality clear sky scene
2019	14 August 2019	S2B_MSIL2A_20190814T062639_T43UEQ	5.3	Cloud mask	Used for NDVI multi-year averaging
2020	5 July 2020	S2A_MSIL2A_20200705T062631_T43UDQ	2.1	Cloud mask	Core scene for anomaly detection
2020	28 August 2020	S2B_MSIL2A_20200828T062639_T43UDQ	8.4	Cloud mask	Seasonal composite integration
2021	15 June 2021	S2A_MSIL2A_20210615T062621_T43UDQ	3.0	Cloud mask, saturation mask	Stable vegetation baseline
2021	3 August 2021	S2B_MSIL2A_20210803T062629_T43UDQ	7.8	Cloud mask	Complementary midsummer scene
2022	22 July 2022	S2A_MSIL2A_20220722T062621_T43UDQ	4.9	Cloud mask	Used for base environmantal modeling
2022	30 September 2022	S2B_MSIL2A_20220930T062619_T43UDQ	6.3	Cloud mask	Final NDVI composite for the year
2023	18 June 2023	S2A_MSIL2A_20230618T062631_T43UDQ	3.2	Cloud mask	High-quality pre-impact conditions
2023	9 August 2023	S2B_MSIL2A_20230809T062639_T43UDQ	9.7	Cloud mask	Final composite, acceptable cloud limit

NDVI was calculated from the near-infrared (R_1, 842 nm) and red (R_2, 665 nm) bands using the standard expression:

$$NDVI = \frac{R_1 - R_2}{R_1 + R_2} \quad (1)$$

For each OTU, average NDVI values were extracted from seasonal composites using variance-elliptical masks (see Figure 5).

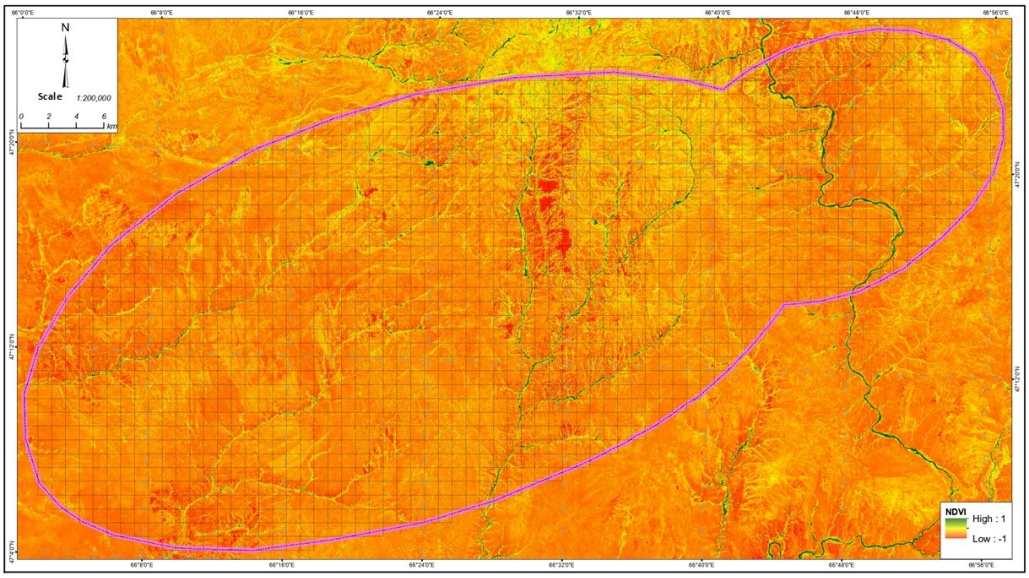


Figure 5. Normalized difference vegetation index.

Then, multi-year composites (2017–2023) were averaged to reduce interannual variability, which allowed us to obtain a "baseline vegetation" layer for IAS analysis.

(4) Determination of soil quality and mechanical strength

Soil parameters were obtained from the national soil and environmental map and converted into two indicators:

(a) Soil quality index (Q_{Bi}): calculated in accordance with the bonitet classification, normalized to a reference humus content of 7% in the 0–50 cm layer and adjusted for salinity, structure, and erosion factors (Table 2) [47].

(b) Soil strength index (Q_{Si}): derived from lithological descriptions and texture classes according to the Protodyakonov scale (GOST 21153.1–75) (Table 3).

Table 2. Soil Quality Correction Coefficients (Bonitet Methodology).

Soil Property	Range/Category	Correction Coefficient	Notes
Humus content (%)	≥7%	1.0	Reference (optimal)
	4–7%	0.8	Typical for chestnut soils
	2–4%	0.6	Degraded humus horizon
	<2%	0.3	Strongly depleted soils
Salinity (EC, dS/m)	<2 (unsalted)	1.0	No correction
	2–4 (lighly salted)	0.7	Moderate yield reduction
	4–8 (moderately saline)	0.5	Strong salinity impact
	>8 (highly saline)	0.3	Severe degradation
Soil structure	Well-aggregated	1.0	Good stability
	Moderately structured	0.8	Typical steppe soil
	Weak structure	0.6	Erosion risk
	Massive/strutureless	0.4	Very low resistance
Erosion class	No erosion	1.0	Optimal
	Slight erosion	0.8	Partial A-horizon removal
	Moderate erosion	0.6	Active erosion processes
	Strong erosion	0.4	Highly degraded

Table 3. Protodyakonov Soil-Strength Categories (Q_{Si}).

Soil/Lithology Type	Protodyakonov Strength (f-Value)	Normalized Coefficient	Notes
Dense Clay, clay loam	3–4	0.9	High mechanical resistence
Loam	2–3	0.8	Typical stable soils
Sandy loam	1–2	0.6	Moderate resistance
Sand (medium/coarse)	0.5–1	0.4	Low stability
Fine sand/dust/loess	<0.5	0.2	Easily disturbed
Saline crust soils	variable (0.3–1)	0.3	Unstable, brittle
Gravelly substrate	4–6	1.0	Very high stability

Mixed soil polygons crossing several OTUs were resolved by area-weighted averaging of the corresponding attributes. All parameters obtained were rasterized and recalculated to an accuracy of 30 m to match other IAS input data. Detailed results and spatial representations are presented (Figure 6).

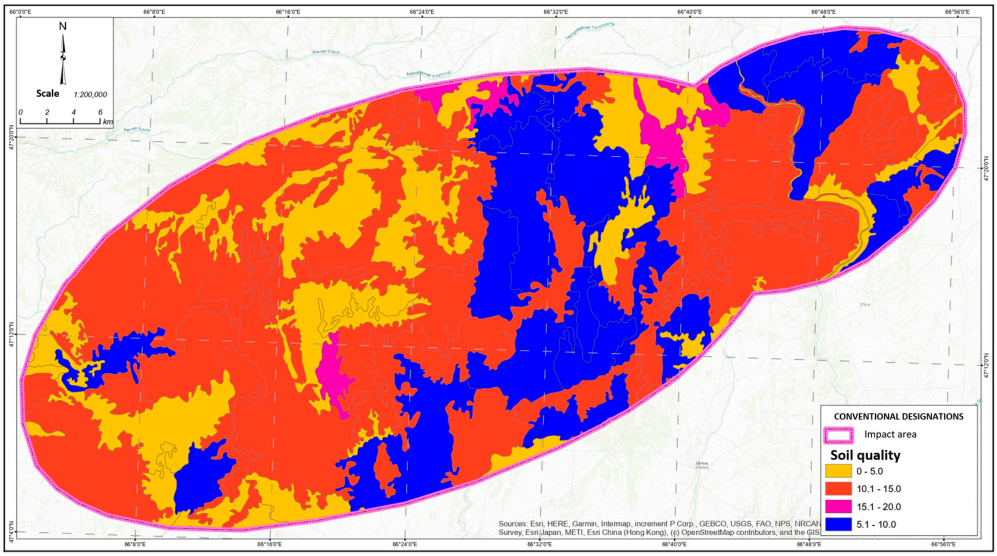


Figure 6. Soil quality and fertility map.

The composite map shows how the modeled impact areas intersect with different types of ecosystems-steppe grasslands, shrub communities, salt marshes, and dry valleys.

This overlay provides a spatial understanding of which landscape components are most vulnerable to potential disturbance.

In areas where the ellipses intersect with surface water bodies or hydrologically active depressions, additional restrictions were imposed on the choice of planting sites, as these features significantly increase the risk of pollutant migration.

Similarly, areas containing dense or recovering vegetation cover were marked as environmentally sensitive, while degraded or sparsely vegetated areas were considered potentially stable under controlled descent scenarios. This integration ensures that both physical (size, shape, orientation) and ecological (type of soil and vegetation cover, slope, hydrological conditions) characteristics are available for multi-criteria assessment.

Thus, geometric and ecological characteristics serve as a link between the ballistic model and the ecological analysis module. This allows IAS to translate the geometry of physical dispersion into quantitative environmental indicators, forming the basis for assessing the stability and ranking of OTUs.

4. Research Results

The research was conducted within the Yu-24 impact zone (impact zones No. 15 and 25) located in the Ulytau district of the Karaganda region, Republic of Kazakhstan.

This area is one of the most studied impact zones for Proton rocket stages launched from the Baikonur cosmodrome.

The region is characterized by slightly undulating steppe plains with absolute heights ranging from 200 to 400 m above sea level, interspersed with shallow depressions and ephemeral streams.

The landscape consists mainly of dry steppe vegetation on chestnut and light chestnut soils with local manifestations of saline and saline complexes.

In climatic terms, this area belongs to the arid continental belt, experiencing strong seasonal contrasts—hot, dry summers and cold winters—which greatly affect vegetation productivity and susceptibility to fires. The spatial extent of the selected study area and its topographic context are shown in Figure 7.

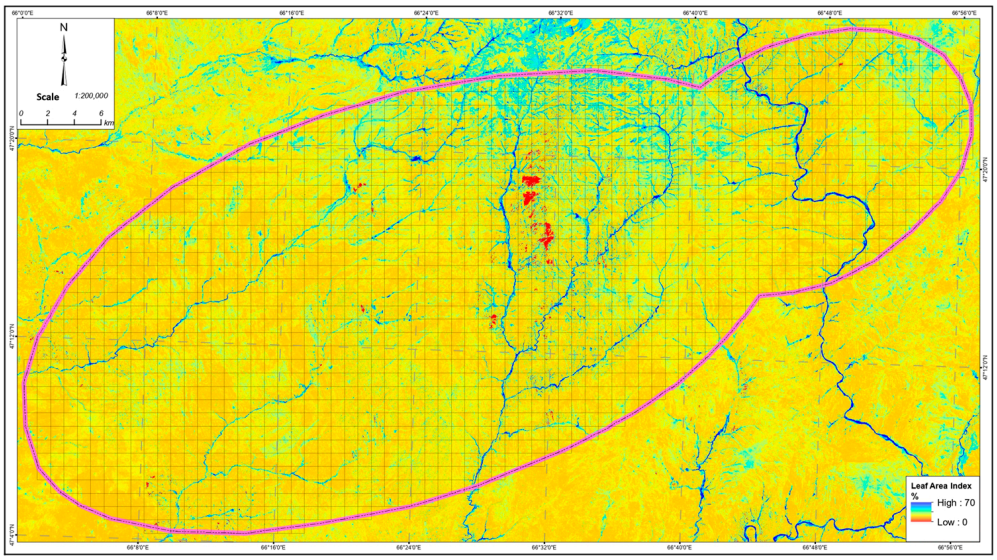


Figure 7. Projected coverage in accordance with LAI (Leaf Area Index).

This figure shows the administrative boundaries, hydrographic network, major landmarks, and coordinate grid used for spatial referencing of all subsequent datasets. Each OTU acts as a separate analytical cell for which all ecological and engineering–geological parameters were calculated. This grid structure ensures compatibility between data with different spatial resolutions and allows for automated statistical extraction of indicators in the IAS environment. The grid was formed using the Baikonur coordinate system (UTM Zone 43 N, EPSG: 32643) with subsequent referencing to the topographic base map.

4.1. Zoning and Formation of OTUs

The delineation of operational-territorial units is the spatial basis for integrating the results of ballistic modeling, remote sensing analysis, and environmental assessment within the IAS. At this stage, a consistent analytical grid is created, allowing for quantitative comparison of diverse environmental parameters. The OTU was designed in accordance with the principles of spatial homogeneity and functional relevance.

Each OTU is an elementary landscape-analytical unit characterized by uniform features of relief, soil, and vegetation. The zoning scheme takes into account the following:

- The boundaries of dispersion ellipses obtained by Monte Carlo modeling;
- The main landforms and drainage lines obtained from a digital elevation model;

- The boundaries of soil cover and soil extracted from thematic maps.

These criteria ensure that each OTU corresponds to a discrete combination of natural-geographical and anthropogenic factors affecting the stability of potential planting sites.

4.2. Assessment and Classification of OTU

4.2.1. Vegetation and Fire Safety (Q_{Vi}, Q_{Fi})

Vegetation is a key indicator of environmental stability in impact zones. Its condition reflects the ecosystem's ability to withstand and recover from mechanical and pyrogenic impacts caused by falling launch vehicle fragments. Within the IAS, vegetation parameters are represented by the vegetation stability coefficient (Q_{Vi}), obtained from Sentinel-2 multispectral images processed for the 2017–2023 growing seasons.

After radiometric and atmospheric correction, multi-temporal composites were obtained for different phenological stages, allowing for the assessment of seasonal and interannual variability. The normalized difference vegetation index (NDVI) was calculated using the red (665 nm) and near-infrared (842 nm) channels.

For each OTU, NDVI statistics were extracted from raster composites using the OTU grid. Spatial NDVI maps illustrating vegetation density and vitality are presented in Figure 8. NDVI data were classified into five qualitative categories, ranging from sparse or degraded vegetation to dense perennial grass-shrub communities. This classification served as the basis for assigning Q_{Vi} scores to individual OTUs.

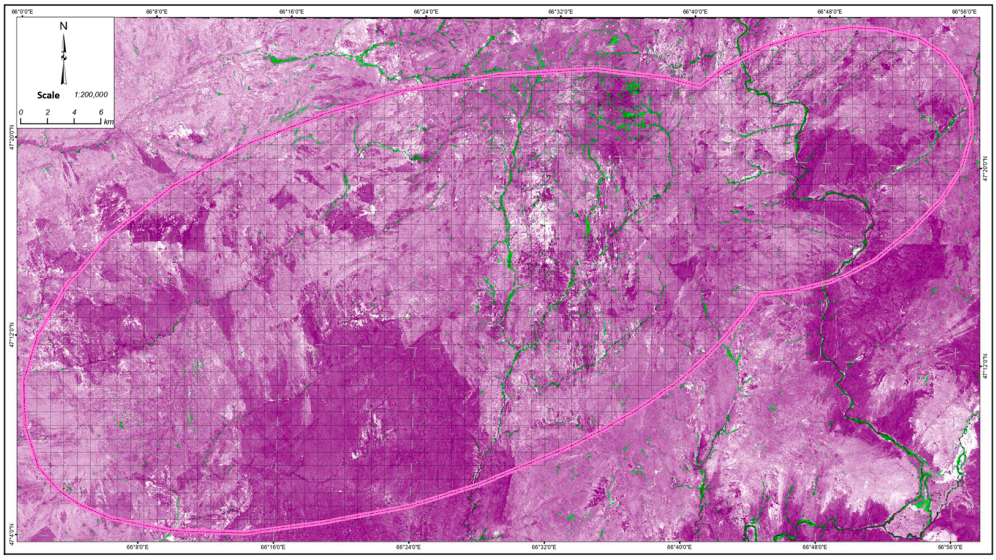


Figure 8. Spatial distribution of fire hazard categories (Q_{Fi} classes) within the Yu-24 impact zone.

According to the thematic zoning (Figure 7), areas with sparse or intermittent vegetation cover are the most resilient, which is associated with their adaptation to extreme conditions and lower biomass. In contrast, areas with dense grass and shrub vegetation are more vulnerable to mechanical impact.

In addition to vegetation analysis, fire safety (Q_{Fi}) is proposed to be taken into account, characterizing the potential for ignition and fire spread within the same spatial framework. For this purpose, the input layer is the density of projective cover and the amount of biomass obtained from NDVI and soil and vegetation cover maps (Table 4 and Figure 7).

Areas with high NDVI values, low moisture retention, and prolonged exposure to drought were identified as potentially high-risk zones, while areas with sparse vegetation or hydrologically buffered areas were classified as low-risk zones (Table 4).

Table 4. Vegetation flammability classification for fire hazard index (Q_{Fi}).

Vegetation Community	Flammability Class	Q_{Fi} Weight	NDVI-Range (Typical)	Rationale
Bare and semi-bare substrate (solonchak, shifting sands, eroded surfaces)	I-non-flammable	0.05	<0.10	Virtually no combustible phytomass; sparse salt-tolerant crusts do not sustain ignition
Sparse halophyte and wormwood (*Artemisia* spp.) communities on saline soils	II-low	0.25	0.10–0.20	Low biomass density; succulent and salt-adapted species have high moisture content and ignite poorly
Mixed-wormwood-fescue (*Artemisia-Festuca*) and wormwood-grass steppe	III-moderate	0.50	0.20–0.35	Moderate standing biomass; dry grass litter in late summer creates continuity of fuel; typical steppe fire risk
Feather-grass. (*Stipa* spp.) and bluegrass (*Poa* spp.) dense steppe communities	IV-high	0.75	0.35–0.50	Dense continuous herbaceous cover; abundant dry litter; rapid fire spread under wind; documented fire foci in the region
Shrub. Communities (*Caragana*, *Spiraea*) and reed/sedge stands near depressions	V-very-high	0.90	0.50–0.65	High woody/semi-woody fuel load; reed beds intensely flammable when dry; fire can smoulder in root litter
Recovering and secondary vegetation on previously disturbed soils (post-impact regrowth)	VI-extreme	1.00	>0.65 (or variable)	Ruderal-pioneer species and dry-standing deadwood from prior fires create maximum fuel continuity and ignition probability

Notes: Q_{Fi}—weight is a normalized coefficient (0–1) used in the composite stability equation (Equation (1)). Higher Q_{Fi} = greater fire hazard = lower OTU stability score. NDVI ranges are indicative for the 2017–2023 growing season composite (Sentinel-2 Level-2A, Sen2Cor. 2.9). Mixed polygons are resolved by area-weighted averaging of Q_{Fi} within each OTU cell (1 × 1 km grid).

The resulting spatial distribution of fire hazard categories is shown in Figure 8.

Vegetation (Q_{Vi}) and fire safety (Q_{Fi}) coefficients were stored as thematic layers in the IAS geodatabase. Each OTU record contains the average NDVI value, the dominant vegetation class, and the corresponding fire hazard category. Together, these indicators characterize the bioecological stability of the territory: dense, moisture-balanced vegetation increases stability, while highly combustible biomass increases pyrogenic vulnerability.

Thus, the combination of the Q_{Vi} and Q_{Fi} layers provides a balanced understanding of how vegetation affects the stability and susceptibility of ecosystems in impact zones. Their comprehensive assessment is the first component of a multi-criteria model of environmental stability.

4.2.2. Soil Quality and Mechanical Strength (Q_{Si}, Q_{Bi})

Soil cover within the study impact zone is one of the key factors determining the mechanical strength and ecological sensitivity of the landing surface. Soils act as a buffer against mechanical deformation and chemical contamination; their properties directly influence the degree of recovery after rocket stage impacts.

Within the IAS, soil conditions are represented by two complementary indices: the ecological quality coefficient (Q_{Bi}) and the mechanical strength coefficient (Q_{Si}).

Ecological quality (Q_{Bi}) was determined using the bonitet (fertility) classification system approved by the Ministry of Agriculture of the Republic of Kazakhstan [47]. For each OTU, soil characteristics were extracted from a digital soil and environmental map (scale 1:200,000), which includes information on humus content, granulometric composition, salinity, carbonate accumulation, and degree of erosion. These parameters are normalized relative to a reference humus content of 7% in the 0–50 cm layer and adjusted by correction factors for mineralization, structure, and thickness of the humus horizon. The resulting QBi values describe the relative fertility and ecological stability of soils within each OTU.

Differentiation of soil types (and soil substrates) is the most common type of engineering calculation. To create a block for assessing the degree of mechanical impact of SRM on various OTUs, the quantitative determination of soil cover diversity is carried out on the basis of digital maps at a scale of 1:200,000—soil and soil-ecological zoning, taken from the ecological passport of the fall area (Figures 9 and 10).

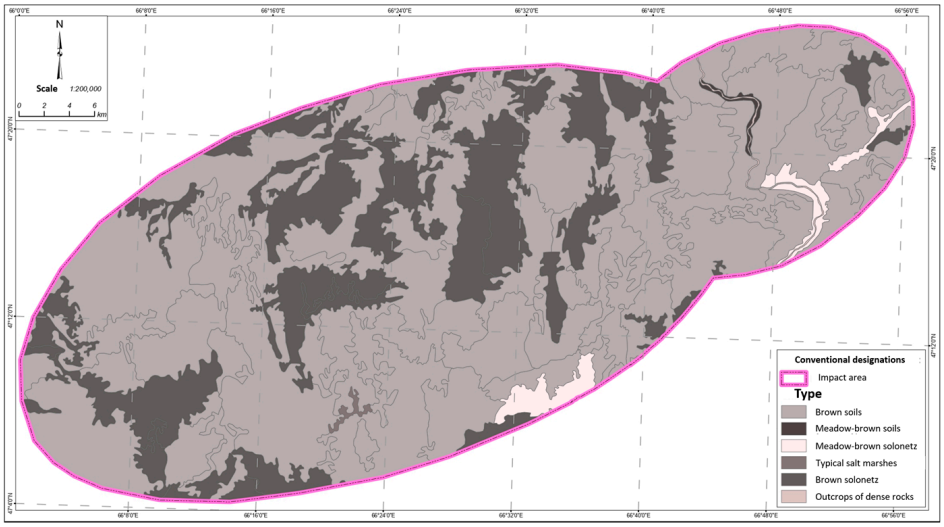


Figure 9. Soil type map.

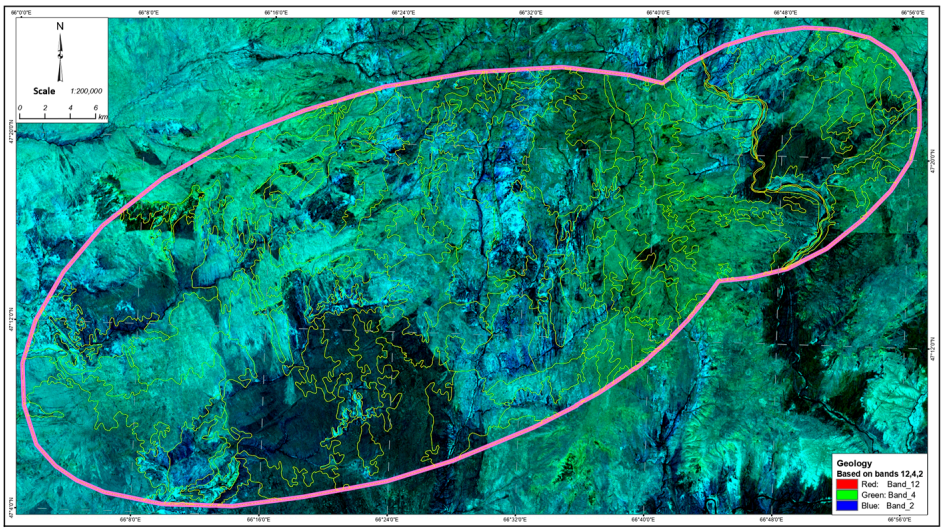


Figure 10. Combining geological bands based on Sentinel-2 data to refine soil map contours.

The digital soil map contains information about soil cover and parent rock. The digital map of soil and ecological zoning uses a multi-stage taxonomic system for dividing the territory. Calculations are performed at the lowest level of soil and ecological zoning—within the boundaries of the catchment areas—in the MapInfo program using the area-weighted average method (Figure 9). The resulting map allows us to identify OTU with the percentage ratio of predominant soil types. If digital maps are available for the study area, the input data for it is calculated using a geoinformation application based on ArcView GIS with Spatial Analyst and 3D Analyst extensions.

The soil cover is characterized by different soil types with different physical and chemical properties. Therefore, it seems appropriate to process the data based on a soil map with already known reference data. The assessment and grading of soil characteristics include the determination of soil bonitet (value) in accordance with standard sorting methods.

The mechanical strength coefficient (Q_{Si}) reflects the ability of the base to withstand mechanical stress without irreversible deformation. It was assessed based on the texture and lithological composition of the soil obtained from the same soil and environmental database and the geological layer of the foundation integrated into the IAS. The classification is compiled according to the Protodyakonov strength scale (GOST 21153.1–75) and distinguishes between stable loamy-clay formations and weakly structured sandy and saline bases.

Each soil polygon was assigned a relative stability class, and area-weighted average values were calculated for OTU cells intersecting several soil types. The resulting QSi map (Figure 10) highlights areas of increased mechanical stability, primarily corresponding to compact loamy soils in the northern and central parts of the study area.

The Q_{Si} and Q_{Bi} layers were combined to obtain a composite soil stability index representing both the physical and ecological aspects of substrate stability. This integrated layer illustrates the spatial differentiation of soil conditions in the impact zone and provides a significant contribution to the overall assessment of OTU stability.

Areas with strong, well-structured soils are considered to be the most stable in terms of mechanical impact and, therefore, more preferable for the fall of step fragments. In contrast, areas with high bonitet indices, characterized by valuable and productive soils, although ecologically stable, are considered more economically vulnerable because their restoration after impact requires significantly higher costs. Degraded, salinated, or loose substrates with low mechanical strength and high ecological sensitivity are identified as areas where rockfall should be avoided or special measures should be taken to prevent and minimize damage.

All soil indicators obtained are stored in the IAS relational database and linked to the corresponding OTU identifiers for analysis of soil parameters in combination with vegetation, fire hazard, and relief characteristics in a multi-criteria environmental assessment.

4.2.3. Relief (Q_{relief})

The morphology of the terrain has a strong influence on both the mechanical distribution of impact energy and the response of the environment to disturbances. Slope gradients and curvature determine the nature of surface runoff, soil erosion potential, and local accumulation of pollutants released after stage separation. Therefore, topography is a critical factor in assessing the environmental sustainability of OTU.

Topographic analysis is performed using the ASTER Global Digital Elevation Model (GDEM, V3) with a spatial resolution of 30 m. From this DEM, slope, exposure, and curvature layers are obtained in IAS using the Spatial Analyst module. The resulting digital elevation model (Figures 11 and 12) illustrates the main landforms in the Yu-24 impact area, ranging from gentle undulating plains to localized ridges and depressions.

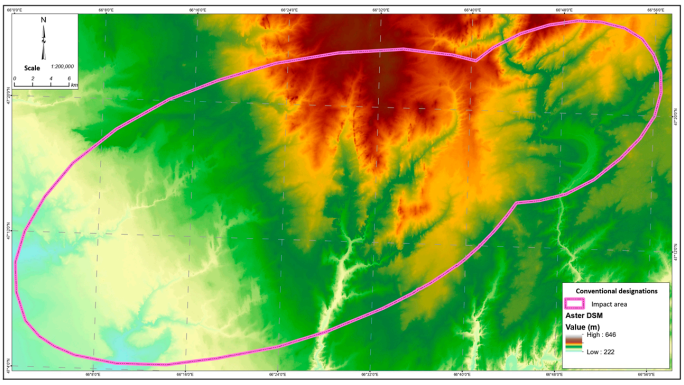


Figure 11. Digital elevation model based on ASTER GDEM data.

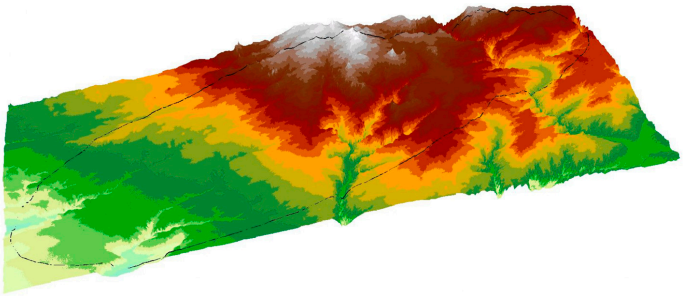


Figure 12. Digital 3D relief model based on ASTER GDEM data.

A surface exposure map (Figure 13) is created to assess the potential effects of solar heating and drying, which affect the moisture balance of vegetation and susceptibility to fires. Areas with southern and western exposures tend to be drier and more prone to erosion, while northern slopes and concave shapes tend to retain moisture and demonstrate greater ecological stability.

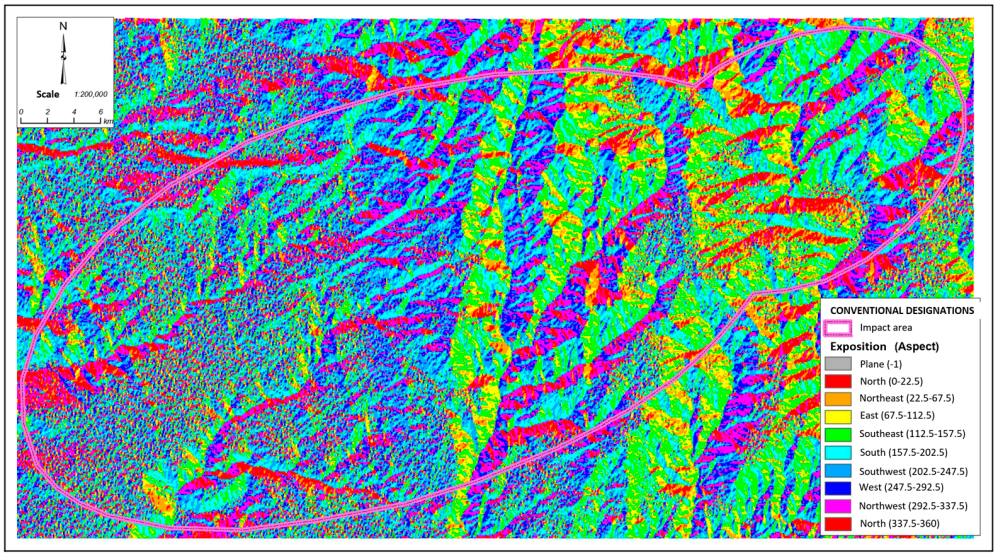


Figure 13. Surface exposure (exposure).

Hydrological structures are extracted from the same DEM using runoff accumulation algorithms and supplemented by manual digitization of watercourses and depressions on topographic maps. This process allows the identification of intermittent channels, ephemeral watercourses, and shallow basins prone to seasonal flooding. The resulting hydrographic network is verified against high-resolution Sentinel-2 images and integrated as a separate vector layer in the IAS.

Special attention is paid to areas where the dispersion ellipses intersect with hydrologically active features such as river valleys or depressions. These intersections are classified as hydrologically sensitive sectors, as potential chemical pollution in these areas can spread along runoff paths and affect larger ecosystems downstream.

The Q_{relief} parameter is obtained by integrating slope, curvature, exposure, and hydrological density within a standardized OTU grid.

Weighting factors are proposed for each factor to reflect their relative impact on stability: steeper slopes and concave shapes reduce the stability rating, while balanced gradients and well-drained profiles increase it. Stable areas, characterized by moderate slopes and low hydrological connectivity, dominate the northern and central parts of the zone, while unstable areas—typically steep or poorly drained depressions—are concentrated along lo-

cal valleys. This differentiation provides important input for determining environmentally safe planting sites.

Thus, the Q_{relief} index represents a terrain relief modifier in the overall environmental sustainability model.

4.3. Integrated Assessment and Ranking of OTUs

To summarize the results of the previous analysis, all environmental indicators—vegetation condition (Q_{Vi}), fire safety (Q_{Fi}), soil mechanical strength (Q_{Si}), soil ecological quality (Q_{Bi}), and relief-hydrological stability (Q_{relief})—are integrated into the IAS structure to obtain a composite environmental stability index for each OTU. The integration procedure follows the logic of weighted superposition, ensuring that indicators with different measurement scales are converted to a common normalized range (0–1).

The overall OTU sustainability index is proposed to be calculated using the following formula:

$$Q_{OTU_i} = \left(k_{V_i}Q_{V_i} + k_{S_i}Q_{s_i} + k_{B_i}Q_{B_i}\right) \times \left(\pm Q_{relief}\right) \quad (2)$$

where Q_{OTUi}—composite sustainability index of the operational-territorial unit (dimensionless, range 0–1); k_{Vi}, k_{Fi}, k_{Si}, k_{Bi}—normalized weight coefficients ($\sum k = 1.00$) reflecting the relative influence of each factor (see Table 5); Q_{Vi}—vegetation condition coefficient; Q_{Fi}—fire hazard coefficient; Q_{Si}—soil mechanical strength coefficient; Q_{Bi}—soil ecological quality coefficient; and Q_{relief}—terrain and hydrological stability modifier (applied as a multiplicative factor; sign reflects stabilizing or destabilizing effect of relief on the composite score).

Table 5. Q_{relief} modifier.

Slope Condition	Curvature Class	Hydrological Condition	Q_{relief} Sign	Interpretation
Mean slope $\leq 5°$	Planar or convex	No watercourse or hydrologically active depression within OTU	+	Stable terrain, well-drained; low erosion and pollutant migration risk; amplifies sustainability score
Mean slope > 5°	Any	Any	-	Elevated runoff velocity and erosion risk; reduces sustainability score
Mean slope $\leq 5°$	Concave	Any	-	Depression morphology; pollutant pooling risk regardless of hydrology
Mean slope $\leq 5°$	Planar or convex	Watercourse, ephemeral channel, or seasonal depression present within OTU	-	Hydrological connectivity increases pollutant spread risk; reduces sustainability score

The sign of the Q_{relief} modifier is determined by a two-threshold classification of the dominant slope gradient within each OTU cell, derived from the ASTER GDEM slope layer. The decision rule is as follows:

- *Positive sign* ($+Q_{relief}$): applied when the area-weighted mean slope within the OTU is $\leq 5°$ and the curvature class is planar or convex, indicating a stable, well-drained surface with low erosion potential and low pollutant accumulation risk. Such terrain amplifies the composite sustainability score.
- *Negative sign* ($-Q_{relief}$): applied when the area-weighted mean slope exceeds 5°, or when the dominant curvature class is concave (hydrological depression), indicating elevated runoff velocity, erosion susceptibility, or pollutant pooling risk. Such terrain reduces the composite sustainability score.

Where a single OTU cell contains both slope classes, the sign is assigned based on the dominant class by area (>50% of cell area). This rule is implemented as a conditional raster operation in the IAS Spatial Analyst module prior to the weighted overlay step (Table 5).

To determine the costs required to restore an operational-territorial unit with an area of Si, the area of damage caused by fire, the fire hazard index is multiplied by the restoration cost coefficient:

$$C_{F_i} = k_F \times Q_{F_i} \tag{3}$$

The rock strength scale [47] is used to calculate the soil strength criterion. For each OTU, the proportion of rocks of different strengths (in percent) is determined, each rock Qp is assigned a weight coefficient, and then the weighted average value is calculated:

$$Q_{si(\text{сред})} = k_1 Q_{p1} + k_2 Q_{p2} + k_3 Q_{p3} + \cdots + k_{n_i} Q_{pn} \tag{4}$$

where n is the number of species present in the Si selected area.

The weighing scheme is derived based on expert assessment calibrated according to literature data on ecosystem resistance and engineering stability [36,43].

For the criterion, the estimated cost of restoration is determined, and then the costs of eliminating damage related to soil strength characteristics are calculated:

$$C_{Q_{p_i}} = C_{p_i} \sum k_{n_i} Q_{np_i} \tag{5}$$

The indicator reflecting the ecological quality (bonitet) of soils is calculated similarly to Formulas (4) and (5). The cost of damage restoration according to this criterion is expressed as

$$C_{B_i} = C_{B_{n_i}} \sum k_{Bi} Q_{Bni} \tag{6}$$

The main reactions of vegetation cover to the fall of PH fragments are a reduction in the projective cover of the soil by plants, up to the complete destruction of the vegetation cover; the death of plants as a result of mechanical impact, fires, and rocket fuel spills; the replacement of dominant and subdominant species with low-productivity communities, etc. [10]. When assessing the state of vegetation cover, an ecosystem approach is used, in which the most important indicators characterizing the degree of disturbance and transformation of vegetation are the parameters of projective cover and species composition. Traditional methods of geobotanical research are used as a methodological basis: description of phytocenoses and spatial distribution of vegetation structure and its relationship with other components of the ecosystem.

The indicator characterizing the state of vegetation cover is determined by the indicators of phytomass and projective cover:

$$Q_{V_i} = n_{V_i} Q_{Vm_i} Q_{PC_i} \tag{7}$$

where n_{V_i} is the weight coefficient determined according to the dominance of the dominant species in the plant community.

Additionally, an indicator is introduced that reflects the rate of ecosystem recovery after mechanical or pyrogenic impact (in points), which is refined as monitoring data accumulates.

Accordingly, the cost of restoration work on vegetation cover is determined as

$$C_{V_i} = n_{V_i} Q_{Vm_i} v_{r_i} C_{nV_i} \tag{8}$$

The total cost of restoring the area Si caused by the listed impacts is determined by summing expressions (4), (6), (7), and (9):

$$C_{\sum i} = C_{S_i} + C_{Q_{Pi}} + C_{Q_{Bi}} + C_{Vi} \quad (9)$$

The optimal zone or OTU area is selected based on the criterion of minimizing total restoration costs.

The economic value (*C*) of each OTU is calculated as follows:

$$C_{impact\ OTU} = C_{OTU_1} + C_{OYU_2} + C_{OTU_3} + \cdots + C_{OTU_n} \quad (10)$$

The main essence of the site selection method is to calculate the total criterion for each territorial unit based on source maps, attribute and reference information.

For each site, the sum of measures ($\sum(Q_f + Q_s + Q_{sk} + Q_{vpc} + Q_{vc})$) of influencing factors falling within the site boundaries is calculated and its estimated value is given.

The territory zoning model is presented in a raster format, in which the economic value and fire resistance of each site are determined and points are assigned in accordance with the developed scoring system. Part of the process is automated by integrating Earth remote sensing data and a geographic information system (cartographic material and corresponding tools).

As a result of applying this methodology, it is possible to significantly reduce the area of the fall zone and increase its functional significance.

The economic efficiency of the proposed methodology is justified by the man-made damage caused to natural ecosystems and the restoration of the biological productivity of disturbed areas.

A schematic representation of the integration workflow is shown in Figure 14, illustrating the flow of data from thematic indicators to the composite stability map.

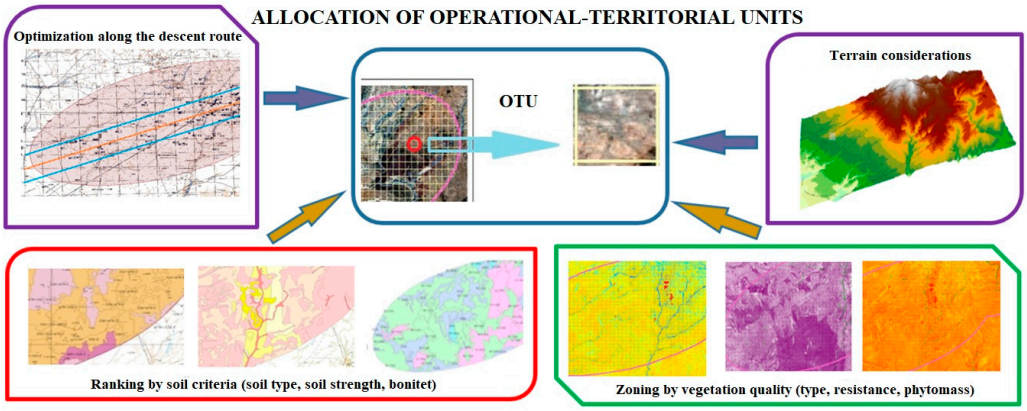


Figure 14. Algorithm for determining OTU.

The composite map obtained is then reclassified into four categories of stability based on quantile thresholds:

(1) High stability—stable areas with favorable vegetation, strong soils, and balanced relief;
(2) Moderate stability—stable but requiring monitoring due to partial degradation;
(3) Low stability—ecologically vulnerable or erosion-prone areas;
(4) Unstable areas—areas combining steep slopes, saline or poor soils, and degraded vegetation cover.

Each OTU is assigned a stability class, recorded in the IAS attribute table, and color-coded on the final output map. The spatial distribution of these ranked OTUs across the

Yu-24 impact area is shown in Figure 15. The figure shows the resulting ecological zoning, which identifies potential landing sites characterized by minimal ecological risk.

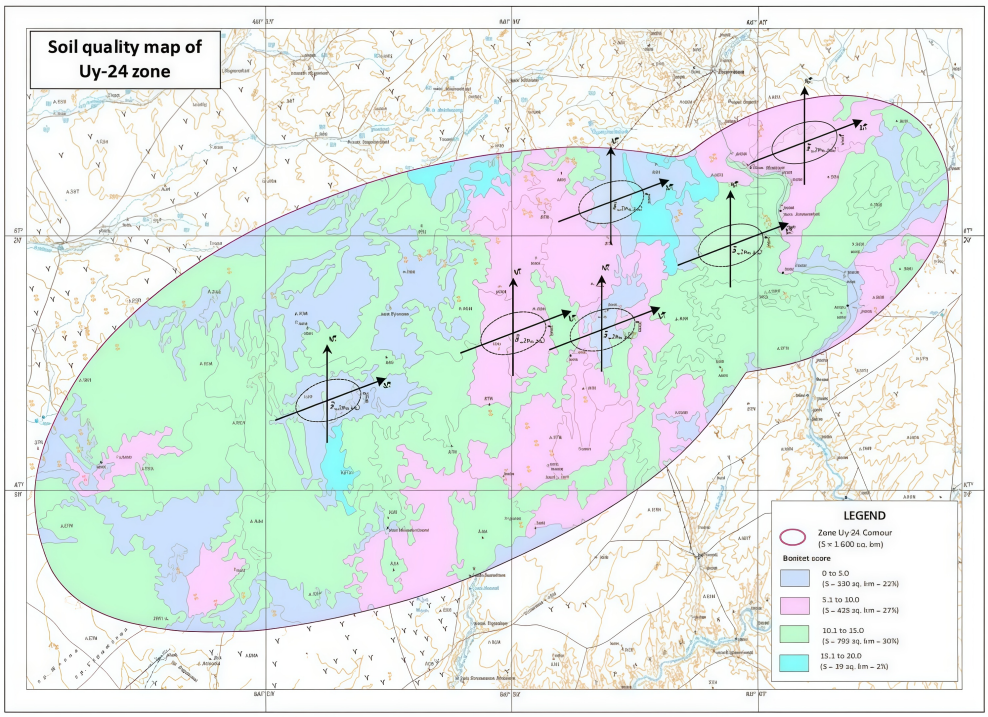


Figure 15. Recommended OTUs.

Analysis of the integrated sustainability map shows clear spatial differentiation. The northern and central sectors of the impact zone demonstrate the greatest sustainability, associated with dense steppe vegetation, loamy soils, and gentle relief. Conversely, the southern and eastern parts show less stability due to the prevalence of saline soils, poorly structured soils, sparse vegetation, and proximity to hydrological depressions. These areas are classified as environmentally vulnerable and are recommended for exclusion from potential landing trajectories or for the application of mitigation measures.

Spatial consistency demonstrates the practical value of integrating environmental data directly into runway design procedures.

The final stage of the analysis consisted of combining all previously calculated environmental and geotechnical indicators—Q_{Vi}, Q_{Fi}, Q_{Si}, Q_{Bi}, and Q_{relief}—into a single OTU assessment framework.

The integration is performed within the IAS, which aggregates all spatial layers and applies a standardized ranking algorithm.

The methodological basis for integration is a composite stability model (Equation (1)), in which the total stability of each OTU is determined as a function of the specified parameters and their corrective weighting coefficients (Table 6).

$$OTUi = (Q_{vegetation} + (Q_{soils} \times B)) \times (\pm Q_{relief}) \quad (11)$$

The algorithm takes into account the interdependence of ecosystem components: for example, the stabilizing effect of dense vegetation can be offset by steep slopes or weak soils, while high soil stability can compensate for partial vegetation degradation.

All normalized input layers (Q_{Vi}, Q_{Fi}, Q_{Si}, Q_{Bi}, and Q_{relief}) are imported into the IAS raster data processing environment and combined using a sequence of weighted overlay operations (Table 7). The resulting integrated map of stable OTUs allows for spatial

differentiation across the entire impact zone, identifying the most ecologically stable and least disturbed areas.

Table 6. Weight coefficients of the composite sustainability index (Normalized expert-derived weights; $\Sigma k = 1.00$).

Index	Indicator	Weight (k)	Weight Distribution	Justification
Q_{Vi}	Vegetation condition (NDVI-based)	0.20	20%	Primary ecological sensitivity indicator; directly reflects ecosystem response to mechanical impact
Q_{Fi}	Fire hazard (flammability index)	0.20	20%	Pyrogenic risk is primary concern at rocket stage impact; directly determines restoration cost coefficient (Equation (3))
Q_{Bi}	Soil ecological quality (bonitet)	0.25	25%	Soil fertility and structure determine long-term recovery capacity; normalized by Kazakhstan Ministry of Agriculture bonitet methodology
Q_{Si}	Soil mechanical strength (Protodyakonov)	0.25	25%	Resistance to crater formation and fragment penetration; critical for estimating physical disturbance extent
Q_{relief}	Relief and hydrological stability	0.10	10%	Slope, aspect, and proximity to water bodies govern fuel migration potential; relatively stable parameter in arid steppe
Total		1.00	Weights based on expert assessment and literature; sensitivity analysis recommended for future validation	

Note: All indicators normalized to [0, 1]. Higher composite score = greater OTU stability. Weights were assigned equal priority to Q_{Vi} and Q_{Fi} given the dominant fire risk in the Yu-24 impact zone. Q_{Bi} and Q_{Si} are equated as complementary soil characteristics. Q_{relief} is assigned a lower weight due to minimal topographic variation in the study area (elevation range 200–400 m, gentle slopes).

Table 7. Distribution of OTUs by composite sustainability class.

Class	Sustainability Level	Score Range (Q_sum)	No. of OTUs	Area, km^2	Share, %	Landscape Characteristics
I	Highly stable	0.75–1.00	~608	~608	~27%	Northern and central sectors; dense steppe vegetation, loamy soils, gentle relief; recommended for controlled descent
II	Moderately stable	0.50–0.74	~878	~878	~39%	Mixed steppe communities, chestnut soils with moderate erosion; acceptable with mitigation
III	Low stability	0.25–0.49	~495	~495	~22%	Southern/eastern parts; saline soils, sparse vegetation, hydrological depressions; exclude from planning
IV	Unstable	0.00–0.24	~270	~270	~12%	Solonchak, shifting sands, ephemeral streams; high fuel migration risk; excluded from descent planning
	Total	-	~2251	~2251	100%	Exact OTU counts to be extracted from IAS raster database

The distribution shown in Table 6 reveals that only approximately 27% of the total impact zone area (Class I, ~608 km^2) meets the threshold for high-stability landing site selection. When Class II areas are included, the combined share of ecologically acceptable territory reaches ~66%, leaving ~34% of the zone (Classes III and IV) excluded from operational planning due to saline soils, sparse vegetation cover, hydrological depressions, and high fuel migration risk. This differentiation demonstrates that the IAS ranking system is responsive across the full range of environmental conditions—from the dense steppe vegetation of the northern sectors to the unstable solonchak and shifting sands of the southern and eastern parts of the impact zone. The practical implication is that

pre-launch selection of descent coordinates within Class I–II OTUs could substantially reduce the ecologically sensitive footprint of rocket stage landings without compromising the operational boundaries of the impact ellipse.

5. Discussion

The results presented in Section 4 demonstrate that the developed IAS provides a practical and quantitative basis for optimizing the ground fall zones of launch vehicles at the Baikonur Cosmodrome.

The developed methodology demonstrates its effectiveness through a structured and reproducible workflow that combines engineering and environmental criteria into a single analytical framework. Rather than relying on numerical results, its value lies in the coordination and logical integration of multiple spatial, environmental, and technical datasets to ensure environmentally sound decisions are made at the earliest stages of planning.

Compared to traditional approaches that define impact zones solely by trajectory and safety limits, the proposed IFRS-based framework introduces environmental sustainability as a determining factor in operational planning. It combines vegetation condition (Q_{Vi}), soil stability (Q_{Si}, Q_{Bi}), relief (Q_{relief}), and fire risk (Q_{Fi}) to identify areas that can absorb or recover from anthropogenic disturbances with minimal long-term degradation.

By synthesizing remote sensing, GIS, and environmental monitoring data, the methodology provides the following:

- Transparent logic for ranking OTUs according to ecosystem sustainability;
- Compatibility with existing flight safety and control systems;
- Scalability, allowing it to be adapted for other ground-based spaceports outside Baikonur.

From an operational perspective, the system improves the efficiency of environmental decision-making by

- Establishing objective and reproducible criteria for selecting landing zones;
- Supporting pre-launch planning and environmental cleanup procedures;
- Enabling periodic monitoring and adjustment of landing point coordinates as environmental conditions change.

The effectiveness of the proposed approach should be considered methodological rather than quantitative—it ensures that environmental safety is embedded in the very logic of launch planning. This integrative design positions IAS as a technological and environmental tool for the sustainable management of launch vehicle fall zones.

Existing international practices for determining rocket launch fall zones are primarily focused on flight safety and aerospace logistics, with limited consideration of environmental parameters. Typical methodologies, such as those used in the United States, the European Union, Japan, India, and Brazil, use trajectory modeling and probabilistic modeling to determine marine or uninhabited land fall zones. These models ensure the safety of populated areas but rarely assess the vulnerability of the ecosystem in the landing zone. As a result, environmental protection remains reactive, relying on mitigation rather than proactive prevention.

The work in [36] illustrates this engineering-oriented paradigm. This work focuses on trajectory management, statistical dispersion, and hazard radius calculation, but it does not include geospatial environmental indicators or data-driven environmental assessment.

In contrast, the methodology presented in this paper integrates environmental sustainability factors into the same decision space traditionally used for flight safety calculations.

The proposed information and analytical system extends the logic of area modeling by incorporating environmental data—vegetation condition (Q_{Vi}), fire risk (Q_{Fi}), soil quality

(Q_{Bi}), soil strength (Q_{Si}), and hydrological stability of the terrain (Q_{relief})—directly into the spatial structure of the impact zone design.

Such integration transforms the decision-making process from a purely mechanical optimization task into a multi-criteria environmental assessment.

An important aspect of the practical application of the IAS is the consideration of the temporal dynamics of environmental indicators. Although the satellite data used in the study represent averaged conditions for the period 2017–2023, the system allows for regular updating of the input layers as new remote sensing data become available. Indicators that are sensitive to interannual variability—such as vegetation condition and fire danger (Q_{Vi}, Q_{Fi})—should be updated annually, since even in arid steppe ecosystems significant deviations may occur due to droughts, abnormal precipitation, or seasonal fires. Conversely, characteristics that change much more slowly, including soil quality (Q_{Bi}) and soil mechanical strength (Q_{Si}), require revision only once every 5–7 years or following substantial anthropogenic disturbances. Relief and hydrological parameters (Q_{relief}) are generally stable and need to be updated only after extreme events that cause erosion or redistribution of surface runoff. This differentiated updating scheme enables the IAS to remain up-to-date without excessive data processing while preserving the reproducibility and operational efficiency of environmental assessments.

The proposed approach differs from previous ones in several key aspects:

- Interdisciplinary synthesis combines aerospace trajectory modeling with environmental GIS analysis in a single modular platform;
- Quantitative mapping of the environment by assigning normalized sustainability coefficients to discrete operational-territorial units;
- Transparency of decision-making allows you to reproduce and verify the ranking of potential landing sites;
- Adaptability—easy integration of new datasets, indicators, or launch configurations without changing the system architecture.

These innovations allow environmental and technical specialists to work within a common spatial interface, ensuring that environmental safety is considered alongside ballistic feasibility.

Consequently, the IAS adapts international principles to specific regions, enabling inland launch sites to carry out sustainable flight range planning in line with global policy objectives.

Thus, the approach presented complements and extends existing international methodologies by introducing a reproducible, environmentally sound decision support system. It does not replace traditional safety modeling but enriches it with spatially explicit environmental intelligence. Thanks to IAS, environmental sustainability becomes an integral part of the engineering design process, rather than an external constraint assessed after launch planning.

This distinction defines the methodological contribution of this study to prevailing international practice.

From a scientific point of view, the work establishes a clear conceptual and computational link between flight safety modeling in the aerospace industry and environmental sustainability assessment.

The proposed IAS architecture provides a verifiable framework for integrating heterogeneous spatial data—remote sensing, digital soil mapping, meteorological, and topographical information—into a coherent decision support system.

From an applied perspective, the methodology provides a framework for adaptive land use management within existing impact zones.

The results obtained emphasize that sustainable space operations require a balance between engineering feasibility and environmental responsibility. IAS demonstrates that these considerations can coexist within a single spatial analysis environment without compromising launch safety or environmental protection.

In summary, the study presents a consistent and verifiable methodology that links data collection, environmental modeling, and decision support into a single workflow.

This confirms the feasibility of integrating environmental sustainability criteria into range planning procedures at ground launch facilities.

The results obtained during the research showed that solving the problem of optimizing impact zones is an original approach in terms of reducing the environmental impact on the biogeocenoses of the rocket launch areas, creating operational reserves of landing points for spent stages, and monitoring these points.

The significance of the research results lies in reducing the technogenic pressure of rocket launches from the Baikonur cosmodrome on landing sites in neighboring countries (Russia, China, Turkmenistan), preserving natural landscapes, natural monuments, specially protected natural areas, preventing fires, and ensuring compliance with the recommendations of international organizations COPUOS and IADC on reducing man-made environmental pollution. The creation of the IAS will make it possible to form a new direction in research on information processing and image recognition, as well as in the development of control systems for launch vehicle onboard systems.

The developed IAS and methodology for predicting the selection of fall areas are highly scalable and can be adapted to other spaceports located in continental areas. In particular, the methodology is applicable for optimizing environmental safety in the fall areas of stages at the following spaceports: Russia (Plesetsk, Baikonur (3rd stage fall zones), Vostochny), China (Jiuquan, Taiyuan), India (Satish Dhawan Space Centre), Iran (Semnan), and Brazil (Alcântara).

Unlike sea launch sites (e.g., Cape Canaveral, Vostochny for eastern launches, Kourou), where stages fall into the ocean, land-based launch sites place a high burden on ecosystems and require geo-ecological management.

6. Research Limitations

The methodology is limited by the absence of empirical validation data. Results should be interpreted as a proof-of-concept.

Although the proposed IAS methodology and architecture have demonstrated consistency and logical integration, a number of limitations currently restrict their applicability.

For example, the spatial resolution of the base datasets, particularly the 30-m DEM and 10-m Sentinel-2 images, limits the accuracy of small-scale analysis in heterogeneous landscapes. This resolution is sufficient for regional planning but may not capture microrelief features or small erosion forms that affect local stability.

The analysis was limited to one representative fall area (Yu-24, fall areas No. 15 and 25) within the Baikonur Cosmodrome polygon. Consequently, the conclusions reflect regional geomorphological and climatic conditions and should not be generalized to all internal launch sites without further verification.

The weighting factors proposed for use in the composite stability equation (Equation (1)) are based on expert estimates and literature references and are only applicable when ranking by superimposing a regular grid. The analysis is based on multi-year averaged conditions for 2017–2023, which smooth out interannual extremes. Therefore, short-term anomalies such as droughts, storms, or fires are underrepresented in the stability assessment. The integration of environmental data into space launch planning is still in its early stages in national practice. The study did not include legal, procedural, or interagency aspects of data

sharing that could affect the practical implementation of this approach in official decision-making processes. Further ground-based research is needed to verify the accuracy of the sustainability assessment of different OTUs and empirically test weighting coefficients using field measurements of vegetation cover, soil compaction, and erosion resistance. These limitations primarily affect the spatial accuracy and temporal responsiveness of the model, rather than its conceptual validity. For example, uncertainty in the weighting scheme may alter local OTU rankings but does not change the overall pattern of high- and low-stability zones. The current structure should be viewed as a methodological justification for integrating environmental criteria into the design of rocket launch zones.

Through gradual improvement of the input data, such as the overlay of a map of red-listed animal migration, the IAS can become a practical tool for supporting real-time environmental decision-making and adaptive management of impact zones.

7. Conclusions

The study presents a conceptual and methodological framework for optimizing ground-based rocket launch zones by integrating geoinformation analysis, remote sensing, and environmental assessment within the IAS.

The proposed approach shifts the focus from environmental rehabilitation after launch to proactive planning based on objective spatial data. By combining ballistic modeling with environmental criteria such as vegetation sustainability, soil strength, terrain features, and fire hazard, the methodology is designed to support the informed selection of potential landing zones with the aim of minimizing environmental disruption while maintaining operational safety.

The main scientific contributions of this work are as follows:

- Formalization of environmental resilience criteria as applied to impact zone optimization;
- Development of a modular IAS architecture that links remote sensing data, environmental parameters, and ballistic modeling;
- Presenting a systematic decision support workflow designed to be adaptable to other inland spaceports.

Although the study focuses on the specific case of the Baikonur spaceport, the proposed methodology is intended to be extensible to other facilities. Its modular design is structured to accommodate updated datasets, higher resolution models, and site-specific calibration as new information becomes available. For example, animal migration maps, etc., could be additionally utilized.

At the same time, the study acknowledges that the results obtained represent a methodological proof of concept rather than a final operational system. Validation using additional launches, refined input data, and extended field verification will be important to confirm the predictive capability of the model and quantify its environmental and operational benefits.

Thus, the presented concept provides a preliminary scientific basis for integrating environmental safety into the early stages of launch planning. It presents a step toward the development of sustainable and responsible space operations by introducing a reproducible, data-driven approach to managing the environmental footprint of rocket launches.

Author Contributions: Conceptualization, G.Y.; methodology, G.Y.; software, N.S.; validation, N.S., E.Y. and G.Y.; formal analysis, G.Y.; investigation, G.Y., N.S. and E.Y.; resources, N.S. and A.Y.; data curation, G.Y. and A.Y.; writing—drafting the original manuscript, G.Y.; writing—reviewing and editing, E.Y.; visualization, N.S. and G.Y.; supervision, G.Y.; project management, A.Y.; acquisition of funding, A.Y. and G.Y. All authors have read and agreed to the published version of the manuscript.

Funding: The research was funded by grants from the Committee of Science of the Ministry of Science and Higher Education of the Republic of Kazakhstan: BR24992839 "Investigation of the impact of ecotoxicants and innovative agrotechnologies on agricultural lands and products in the Kostanay Region," AP19679969 "Study of identification processes of rocket hydrocarbon fuels in soils of carrier-rocket operation areas and development of their hygienic standards," and AP09258759 "Development of an information–predictive system model for determining launch and fall areas of ultralight carrier rockets in compliance with environmental safety requirements.

Data Availability Statement: The data supporting the findings of this study were obtained from a combination of open and institutionally collected sources. Satellite data used for vegetation and environmental analysis were obtained from the Copernicus Sentinel-2 mission and are publicly available through the European Space Agency (ESA) Copernicus Open Access Hub (https://dataspace.copernicus.eu/). Digital elevation models (DEMs) were created using Copernicus DEM and SRTM datasets, which are publicly available through open geospatial data portals. Geospatial and environmental field data on rocket stage fall zones were collected as part of research projects conducted by the Ministry of Science and Higher Education of the Republic of Kazakhstan. These datasets are available from the corresponding author upon reasonable request, subject to confidentiality restrictions related to space infrastructure deployment and environmental monitoring agreements. Sentinel-2 pre-processing was performed in ESA SNAP 9.0 with Sen2Cor 2.9. Spatial analysis, raster processing, and map generation were performed in ArcGIS Pro 3.x (ESRI, Redlands, CA, USA).

Acknowledgments: The authors would like to thank the reviewers for their valuable and constructive feedback on this manuscript.

Conflicts of Interest: Author Elmira Yermoldina was employed by the company Branch Office of the Republican State Enterprise "Infracos". The remaining authors declare that the research was conducted in the absence of any commercial or financial relationships that could be construed as a potential conflict of interest.

Abbreviations

The following abbreviations are used in this manuscript:

GIS	Geographic information system
IA	impact area
IAS	information and analytical system
ILV	integrated launch vehicle
LPRE	Liquid Propellant Rocket Engines
LV	launch vehicles
OTU	operational-territorial units
RFC	rocket fuel components
SS	spent stage
NDVI	Normalized difference vegetation index

References

1. Lednev, S.; Koroleva, T.; Krechetov, P.; Sharapova, A.; Semenkov, I.; Karpachevskiy, A. Revegetation of areas disturbed by rocket impact in Central Kazakhstan. *Écoscience* **2017**, *25*, 25–38. [CrossRef]
2. Kopack, R.A. Rocket Wastelands in Kazakhstan: Scientific Authoritarianism and the Baikonur Cosmodrome. *Ann. Am. Assoc. Geogr.* **2019**, *109*, 556–567. [CrossRef]
3. Government of the Republic of Kazakhstan. Resolution No. 313 of May 23, 2019. Agreement on Cooperation in Launching Soyuz-2 Launch Vehicles from Baikonur. Available online: https://adilet.zan.kz/rus/docs/P1900000313 (accessed on 11 May 2026).
4. Dallas, J.A.; Raval, S.; Alvarez Gaitan, J.P.; Saydam, S.; Dempster, A.G. The environmental impact of emissions from space launches: A comprehensive review. *J. Clean. Prod.* **2020**, *255*, 120209. [CrossRef]

5. Ryan, R.; Marais, E.A.; Balhatchet, C.; Eastham, S.D. Impact of Rocket Launch and Space Debris Air Pollutant Emissions on Stratospheric Ozone and Global Climate. *Earth's Future* **2022**, *10*, e2021EF002612. [CrossRef]
6. Byers, M.; Byers, C. Toxic splash: Russian rocket stages dropped in Arctic waters raise health, environmental and legal concerns. *Polar Rec.* **2017**, *53*, 580–591. [CrossRef]
7. Carlsen, L.; Kenesova, O.A.; Batyrbekova, S.E. A preliminary assessment of the potential environmental and human health impact of unsymmetrical dimethylhydrazine. *Chemosphere* **2007**, *67*, 1108–1116. [CrossRef] [PubMed]
8. Koroleva, T.V.; Semenkov, I.N.; Sharapova, A.V.; Krechetov, P.P.; Lednev, S.A. Ecological consequences of space rocket accidents in Kazakhstan between 1999 and 2018. *Environ. Pollut.* **2021**, *268*, 115711. [CrossRef] [PubMed]
9. Koroleva, T.V.; Krechetov, P.P.; Semenkov, I.N.; Sharapova, A.V.; Lednev, S.A.; Karpachevskiy, A.M.; Kondratyev, A.D.; Kasimov, N.S. The environmental impact of space transport. *Transp. Res. D* **2018**, *58*, 54–69. [CrossRef]
10. Maikanov, B.S.; Auteleyeva, L.T.; Zhubatov, Z.K.; Terlikbayev, A.A.; Kamsaev, K.M. The Effect of an Accidental Carrier Rocket Crash on Soil and Vegetation Cover. *J. Ecol. Eng.* **2022**, *23*, 176–184. [CrossRef]
11. Barmin, I.V.; Neustroev, V.N.; Lebedeva, L.I. Problems of ground safety supporting at launch of space vehicle with manned spacecraft. *Acta Astronaut.* **2018**, *150*, 6–14. [CrossRef]
12. Novikov, V.K.; Novikov, S.V.; Tatarinov, V.V. Possible directions for reducing the influence of the rocket and space industry on the environment. *AIP Conf. Proc.* **2019**, *2171*, 100003. [CrossRef]
13. Vinogradov, Y.A.; Asming, V.E. Detection of Impact Points of Spent Launch Vehicle Stages Using Infrasound. *Seism. Instrum.* **2018**, *54*, 387–400. [CrossRef]
14. Decree of the President of the Republic of Kazakhstan Dated April 17, 1995 No. 2195 "On Ratification of the Lease Agreement for the Baikonur Complex between the Government of the Republic of Kazakhstan and the Government of the Russian Federation". Available online: https://adilet.zan.kz/rus/docs/U950002195_ (accessed on 11 May 2026).
15. Atygayev, A.B.; Mukanova, G.A.; Bazarbayeva, T.A.; Kurbatova, N.V.; Zubova, O.A.; Yerekeyeva, S. Study of the Effect of Rocket Fuel on Plant Communities. *J. Ecol. Eng.* **2021**, *22*, 172–181. [CrossRef]
16. Dominguez Calabuig, G.J.; Miraux, L.; Wilson, A.R.; Sarritzu, A.; Pasini, A. Eco-design of future reusable launchers: Insight into their life cycle and atmospheric impact. In *Proceedings of the 9th European Conference for Aeronautics and Space Sciences (EUCASS)*; EUCASS Association: Brussels, Belgium, 2022. [CrossRef]
17. Maury, T.; Serrano, S.-M.; Loubet, P.; Sonnemann, G.; Colombo, C.; Innocenti, L. Space debris through the prism of the environmental performance of space systems: The case of Sentinel-3 redesigned mission. *J. Space Saf. Eng.* **2020**, *7*, 198–205. [CrossRef]
18. Environmental Assessment for Falcon 1 and Falcon 9 at Cape Canaveral. Available online: https://apps.dtic.mil/sti/pdfs/ADA611861.pdf (accessed on 6 June 2026).
19. Gaston, K.J.; Anderson, K.; Shutler, J.D.; Brewin, R.; Yan, X. Environmental impacts of increasing numbers of artificial space objects. *Front. Ecol. Environ.* **2023**, *21*, 289–296. [CrossRef]
20. Ross, M.; Toohey, D.; Peinemann, M.; Ross, P. Limits on the Space Launch Market Related to Stratospheric Ozone Depletion. *Astropolitics* **2009**, *7*, 50–82. [CrossRef]
21. Gingerich, D.; Forrest, J.; Abiin, A.; Maricle-Fitzpatrick, T. The Russian R-16 Nedelin Disaster: An Historical Analysis of Failed Safety Management. *J. Space Saf. Eng.* **2015**, *2*, 65–73. [CrossRef]
22. Yefremkov, A.A. Main Directions of Work to Ensure Environmental Safety in Areas of Falling Rocket Parts (In Russian: Основные направления работ по обеспечению экологической безопасности в районах падения отделяющихся частей ракет). *Mir. Nauk. Kult. Obraz. (MNKO)* **2010**, *5*, 248–249. Available online: https://cyberleninka.ru/article/n/osnovnye-napravleniya-rabot-po-obespecheniyu-ekologicheskoy-bezopasnosti-v-rayonah-padeniya-otdelyayuschihsya-chastey-raket-i-raket (accessed on 8 June 2026).
23. Balesdent, M.; Bérend, N.; Dépincé, P.; Chriette, A. A survey of multidisciplinary design optimization. *Struct. Multidiscip. Optim.* **2012**, *45*, 619–642. [CrossRef]
24. Trushlyakov, V.; Shatrov, Y.; Sujmenbaev, B.; Baranov, D. Fire and environmental safety of liquid-propellant launch vehicles. *Acta Astronaut.* **2017**, *131*, 96–101. [CrossRef]
25. Shu, J.; Kim, J.W.; Lee, J.W.; Kim, S. Mission design optimization for launch vehicles. *J. Aerosp. Eng.* **2016**, *230*, 3–18. [CrossRef]
26. Jamilnia, R.; Naghash, A. Optimization of staging and trajectory. *Aerosp. Sci. Technol.* **2012**, *23*, 85–92. [CrossRef]
27. Civek-Coşkun, E.; Özgören, K. A generalized staging optimization program for space launch vehicles. In *Proceedings of the 2013 6th International Conference on Recent Advances in Space Technologies (RAST), Istanbul, Turkey, 12–14 June 2013*; IEEE: Piscataway, NJ, USA, 2013; pp. 857–862. [CrossRef]
28. Edberg, D.; Costa, W. *Design of Rockets and Space Launch Vehicles*, 2nd ed.; AIAA: Reston, VI, USA, 2022. [CrossRef]
29. Brown, T.F.M.; Bannister, M.T.; Revell, L.E. Envisioning a sustainable future for space launches: A review of current research and policy. *J. R. Soc. N. Z.* **2023**, *54*, 273–289. [CrossRef] [PubMed]

30. Zhong, Y.; Liu, D.; Wang, C. Key technologies for reusable launch vehicles. *IOP Conf. Ser. Mater. Sci. Eng.* **2018**, *449*, 012008. [CrossRef]
31. Wu, H.; Zhang, Z. Development of reusable launch vehicles. *Appl. Comput. Eng.* **2023**, *11*, 65–75. [CrossRef]
32. Wilde, P.D. Range safety requirements. *J. Space Saf. Eng.* **2018**, *5*, 14–21. [CrossRef]
33. Trushlyakov, V.I.; Zharikov, K.I.; Lempert, D.B. Development of Solid Gas Generating Compositions to Ensure Non-Explosiveness of Spent Orbital Stages of Liquid Rocket Space Launch Vehicles. *Eurasian Chem.-Technol. J.* **2017**, *19*, 63–70. [CrossRef]
34. Trushlyakov, V.; Shatrov, Y. Improving of technical characteristics of launch vehicles with liquid rocket engines using active onboard de-orbiting systems. *Acta Astronaut.* **2017**, *138*, 19–27. [CrossRef]
35. Akylbek, B.; Gulnaz, Y.; Valery, T.; Maksat, K.; Nurlan, S. Studies on the Extraction of the Guaranteed Fuel Reserve in the Tanks of the Expended Stage. *J. Appl. Fluid Mech.* **2023**, *16*, 1331–1344. [CrossRef]
36. Suimenbayev, B.T.; Trushlyakov, V.I.; Zhubatov, Z.K.; Yermoldina, G.T.; Suimenbayeva, Z.B.; Bapyshev, A.M. Optimization of allocation of areas for the falling of the worked-off stages boosters of the launch vehicle based on zoning and classification of the existing impact areas of Baikonur cosmodrome. In *Proceedings of the 8th European Conference for Aeronautics and Space Sciences (EUCASS), Madrid, Spain*; EUCASS Association: Brussels, Belgium, 2019; pp. 89–102. [CrossRef]
37. Mukundan, V.; Maity, A.; Kumar, S.R.; Rajeev, U.P. Terminal descent optimization. *IFAC-PapersOnLine* **2022**, *55*, 37–42. [CrossRef]
38. Toso, F.; Riccardi, A.; Minisci, E.; Maddock, C.A. Optimization of ascent and descent trajectories for lifting body space access vehicles. In Proceedings of the 66th International Astronautical Congress, Jerusalem, Israel, 12–16 October 2015. Available online: https://strathprints.strath.ac.uk/57162/1/Toso_etal_IAC_2015_optimisation_of_ascent_and_descent_trajectories.pdf (accessed on 6 June 2026).
39. Trushlyakov, V.; Lesnyak, I.Y.; Urbansky, V.A. Formation of requirements to the laboratory experimental unit under condition of continuation of researches of processes of heat and mass transfer on a model experimental unit. *J. Phys. Conf. Ser.* **2021**, *1791*, 012027. [CrossRef]
40. Kapelyushin, Y.; Lazorak, R.; Peshkov, R.; Trofimov, E. Methods for calculation of drop regions. *Aerospace* **2023**, *10*, 424. [CrossRef]
41. Nam, Y.-W.; Seong, T.; Ahn, J. Adjusted instantaneous impact point. *J. Spacecr. Rocket.* **2016**, *53*, 766–773. [CrossRef]
42. Alipbayev, K.A.; Yermoldina, G.T.; Bapishev, A.M.; Aden, A.E. Modernization of the Information and Analytical System of the Crash Areas of the Baikonur Cosmodrome during the Controlled Descent of the Spent Stage of the Launch Vehicle. In *Proceedings of the 2021 International Conference on Electrical, Communication, and Computer Engineering (ICECCE), Kuala Lumpur, Malaysia, 12–13 June 2021*; IEEE: Piscataway, NJ, USA, 2021. [CrossRef]
43. Cho, B.; Jo, B.U.; Ahn, J. Integrated framework for staging and trajectory optimization. *Int. J. Aeronaut. Space Sci.* **2021**, *22*, 963–973. [CrossRef]
44. Noga, T.; Michałów, M.; Ptasiński, G. Comparison of dispersion methods for sounding rockets. *J. Space Saf. Eng.* **2021**, *8*, 288–296. [CrossRef]
45. Resolution of the Government of the Republic of Kazakhstan Dated December 13, 2005 No. 1242 "On Approval of the Agreement Between the Government of the Republic of Kazakhstan and the Government of the Russian Federation on Ecology and Nature Management on the Territory of the Baikonur Complex Under the Conditions of Its Lease by the Russian Federation". Available online: https://adilet.zan.kz/rus/docs/P050001242_ (accessed on 8 June 2026).
46. *GOST 21153.1-75*; Rocks. Methods for Determining the Strength Coefficient by Protodyakonov. Standards Publishing House: Moscow, Russia, 1975. Available online: https://files.stroyinf.ru/Data2/1/4294852/4294852871.pdf (accessed on 8 June 2026).
47. Order of the Minister of Agriculture of the Republic of Kazakhstan dated October 26, 2022, No. 342. "On Approval of the Methodology for Soil Quality Assessment (Bonitation)." Registered with the Ministry of Justice of the Republic of Kazakhstan on October 28, 2022, No. 30350. Available online: https://adilet.zan.kz/rus/docs/V2200030350 (accessed on 8 June 2026).
48. Semenkov, I.; Koroleva, T. Review on the environmental impact of emissions from space launches: A case study for areas affected by the Russian space programme. *Environ. Sci. Pollut. Res.* **2022**, *29*, 89807–89822. [CrossRef]
49. Ang, L.P.; Kong, F.; Hernández-Rodríguez, E.; Liu, Q.; Cerrej, C.; Feldman, M.J.; Shu, L.; Ye, L.-X.; Gao, L.; Ang, L.L.; et al. Rocket launches threaten global biodiversity conservation. *Commun. Earth Environ.* **2024**, *5*, 799. [CrossRef]

Disclaimer/Publisher's Note: The statements, opinions and data contained in all publications are solely those of the individual author(s) and contributor(s) and not of MDPI and/or the editor(s). MDPI and/or the editor(s) disclaim responsibility for any injury to people or property resulting from any ideas, methods, instructions or products referred to in the content.